ELSEVIER

Applied Surface Science 136 (1998) 298–305

applied surface science

Reduction of the size of the implanted silver nanoparticles in float glass during excimer laser annealing

A.L. Stepanov [a,b], D.E. Hole [b,*], A.A. Bukharaev [c], P.D. Townsend [b], N.I. Nurgazizov [c]

[a] *Lab. of Radiation physics, Kazan Physical–Technical Institute, Sibirsky Trakt 10 / 7, 420029, Kazan, Russian Federation*
[b] *School of Engineering, Pevensey Building, University of Sussex, Brighton, BN1 9QH, UK*
[c] *Lab. of Physical–chemical processes, Kazan Physical–Technical Institute, Sibirsky Trakt 10 / 7, 420029, Kazan, Russian Federation*

Received 20 May 1998; accepted 14 July 1998

Abstract

Silver nanoparticles have been synthesised by ion implantation in float glass at 60 keV to a dose of 7.0×10^{16} ion/cm^2 and a current density of 10 μA/cm^2 at a temperature of 50°C. The size distribution of the metal particles was controlled by monitoring optical transmittance and reflectance together with atomic force microscopy measurements and Rutherford backscattering spectroscopy. A reduction in size of large silver nanoparticles and some dissolution of silver into the glass network has been made by pulse annealing with a high-power KrF excimer laser. The present study explores the possibilities of controlled size formation of metal nanoparticles within an insulator. Explanations of the observed modifications are proposed.

PACS: 78.66.V; 78.66.J; 61.80.B; 81.05.Y; 78.66

Keywords: Silver; Float glass; Ion implantation; Nanoparticles; Optical absorption; Laser annealing; Atomic force microscopy

1. Introduction

Some years ago [1,2] it was shown that Au and Ag nanoparticles were formed by ion implantation in silicate glasses, at concentrations unattainable in any melt-glass fabrication process. The growth of the particles depends on many variables including beam conditions or post-implantation furnace heat treatments. As the field has developed other investigators have found evidence for nanoparticle formation in dielectrics implanted with a variety of metal ions. The optical properties of ion-implanted glasses have been studied extensively by absorption spectroscopy in the visible and infrared portions of the spectrum, for example see Ref. [3]. These experiments have yielded a wealth of information on surface plasmon resonance and of the bond-breaking which occurs as the nanoparticles are accommodated in the implanted layer. Also shown was the possibility of making nonlinear waveguide devices by ion implantation to produce Cu and Au nanoparticles in high-purity fused silica and in sapphire [4]. These metal particles exhibit picosecond nonlinear response times and with

* Corresponding author. Tel.: +44-1273-678193; Fax: +44-1273-678193; E-mail: d.hole@sussex.ac.uk

0169-4332/98/$ - see front matter
PII: S0169-4332(98)00349-3

effective third-order susceptibilities as much as several hundred times larger than those of typical colloidal melt glasses.

The optical properties of material with nanoparticles produced by ion implantation can be controlled to some extent by the local metal concentration, by the formation of alloys of several dopants, or by various thermal treatments [3]. Many of these processes are only moderately well understood, although they have the potential for applications into optical devices and photonics. A major problem is that, as formed, there is invariably a very wide distribution of nanoparticle sizes. Many features, such as the absorption or non-linear response, are size dependent, and hence for any potential application, variations in size degrade the performance, or confuse the interpretation of the fundamental processes.

Ion implantation and high power laser pulse treatments can be used to alter the size of the nanoparticles [5]. Depending on the laser wavelength, power density or pulse length, implanted materials can potentially be modified. It was shown, for example, that laser irradiation in the region of transparency of the glass [visible and infra red], reduces the size of implanted silver particles [6], as the result of a process of photoionization caused by two-photon particle absorption, or changes the internal structure of implanted iron particles [7]. In these experiments the laser light was primarily absorbed by the metal particles. Alternatively annealing of implanted materials can be made with a laser at wavelengths of absorption in the glass (ultraviolet region). Recently data were reported for high-power excimer ArF (193 nm) laser pulses that decreased the reflectance intensity of implanted silver nanoparticles within float glass [8]. In this article it was suggested that after multi-pulse laser treatment of implanted glass, either the silver particles were converted into atoms, or the large particles were separated into such small units that they no longer interact as particles. In principle, there is also a possibility for evaporation of silver from the surface of glass during laser annealing [9]. Our present work aims to continue the study of excimer (KrF) laser interactions with glass containing metal nanoparticles, and in particular, addresses the questions regarding the change in size or total dissolution of silver nanoparticles under high pulse laser treatment.

2. Experimental

The implantation of float glasses has been performed with Ag^+ ions at 60 keV, to a dose of 7.0×10^{16} ion/cm^2 at a beam current density of 10 μA/cm^2 using a Whickham ion implanter. The bulk temperature of the sample was monitored and controlled between 45 and 55°C during the implantation. All implantations were carried out in a controlled vacuum of 10^{-5} mbar. Approximate chemical composition of the float soda–lime silica glass (from Societa Italiana Vetro) is 70% SiO_2, 20% Na_2O, and 10% CaO. The implantation was made into the side of the glass, which was not in contact with tin bath during the float glass process [10].

Pulsed laser treatment has been used with a KrF excimer laser (ATLEX 210) with a wavelength of 248 nm and pulse length of 17 ns full width at half-maximum, which was partially focused on the sample area of 10×10 mm. Three pulses of equal energy density of 200 mJ/cm^2 were accumulated in the same area of the sample at a repetition rate of 1 s^{-1} to yield a fluence of total 600 mJ/cm^2 which was comparable with total energy power of 500 mJ/cm^2 used in Ref. [8]. Pulse-to-pulse energy variation was typically within $\pm 2\%$. Energy density was determined with a laser power meter model DGX (OPHIR).

Depth analyses were made by Rutherford backscattering spectrometry (RBS) with an analysing beam of $^4He^+$ with an energy of 1.89 MeV, at a total dose of 20 μC using a Van de Graaff accelerator. The backscattering collection angle and detector acceptance angles were $\theta = 150°$ and $\Omega = 0.42$ msr. The energy resolution was 21 keV (≈ 10 nm), under 10 channels and beam currents were limited to about 10 nA, conductive carbon paint was used to control surface charging during analyses.

Optical reflectance and transmittance spectra at normal incidence of the light, with an analysing beam of 4-mm diameter, were recorded with a Monolight optical system in the range from 350 to 800 nm at room temperature. Repeatability of the optical spectra for the analysed samples was about 2%.

Topographic profiling of as-implanted and laser annealed surfaces was performed with atomic force microscopy (AFM) P4-SPM-MDT, working in tap-

ping mode. Vertical displacement of the sensitive cantilever in the microscope was registered by deflection of the lower power laser beam reflected from the probe tip. The highest resolution obtained of the AFM was 0.5 nm both in a surface plane and in the perpendicular direction. The sample was clamped on a tube piezoscanner that provides the scanning area of 3.7×3.7 μm. The constant force operating mode was employed and the conventional feedback loop circuit was used to maintain the constant force at less than 100 nN. The measurements were performed in air.

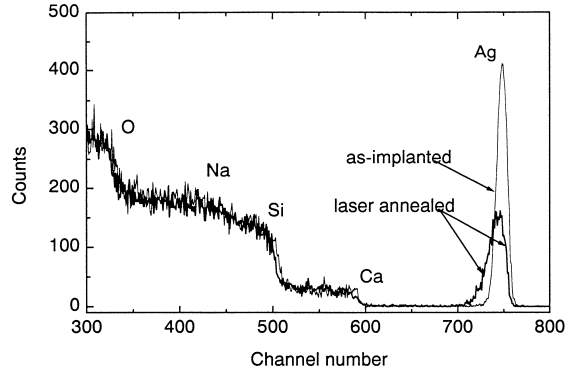

Fig. 2. The RBS spectra for the silver implanted glass before and after laser annealing.

3. Results

The silver ion implantation leads to formation of metal nanoparticles within the thin under-surface layer of float glass [3]. Insulators containing silver nanoparticles show optical absorption determined by collective high-frequency plasma oscillations of the electron gas at the boundary of the metal-insulating interface, called the surface plasmon resonance [11]. Transmittance and reflectance data of as-implanted glass are presented in Fig. 1. The transmission spectrum is characterised by a deep minimum near 430 nm, and the shape of spectral curve is symmetrical (Fig. 1a). The spectrum of reflectivity is more complex and that measured from the implant face of the sample has overlapping peaks from 430 nm at the shoulder in the left part of the spectrum curve to a clearly determined maximum at 490 nm (Fig. 1b). These spectral distributions are typical for samples prepared by ion implantation under similar conditions, for example in Ref. [12].

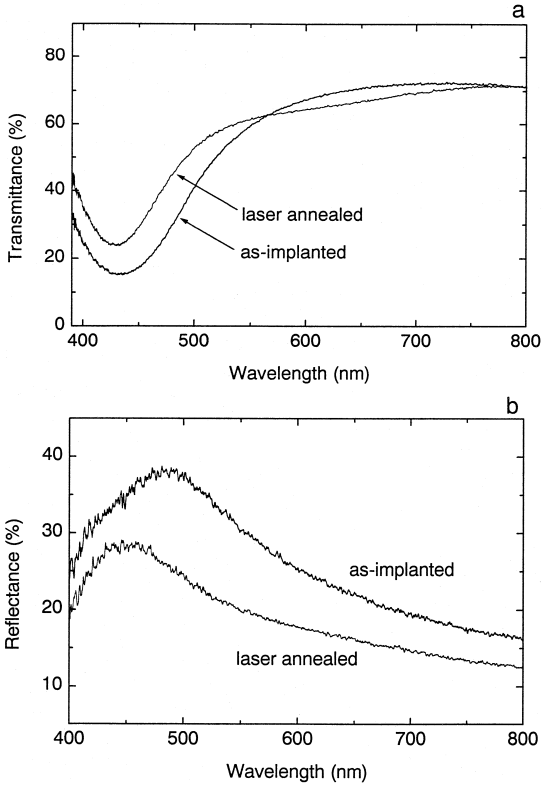

Fig. 1. (a) Transmittance of the silver implanted and laser annealed float glass samples. (b) Reflectance of the silver implanted and laser annealed samples.

High-power pulse laser treatment of the implanted samples has changed their optical spectral characteristics. The location of the transmittance minimum shifts slightly towards shorter wavelengths, and the transmittance in peak position increases from 16 to 23% (Fig. 1a). More remarkable change was found in the reflectance spectra (Fig. 1b), the peak of the overlapping bands shifts continuously from 490 to 450 nm, with modifications in the shape of the envelope of the bands, which becomes narrower. The reflectance intensity falls from 38 to 30%.

RBS data show that the pulse laser treatment causes a loss 30% of the entire silver content in the samples, probably because of evaporation of silver from the surface of sample. The maximum silver atomic concentration occurs at the projected range of

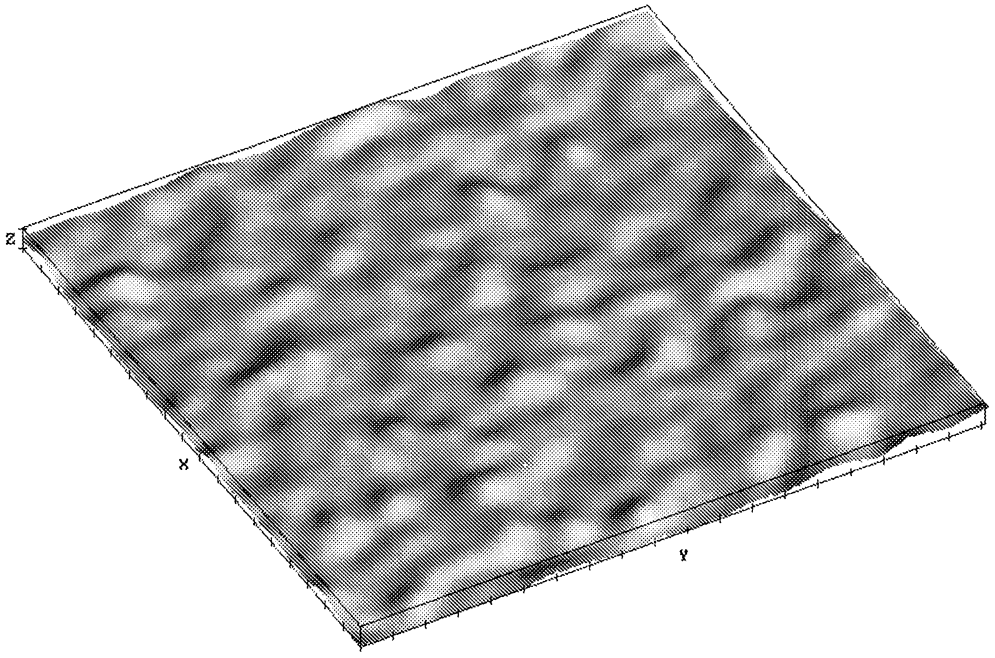

Fig. 3. An AFM image of a silver implanted surface of float glass. The *X* and *Y* scales are 100 nm, and the *Z* scale is 3 nm.

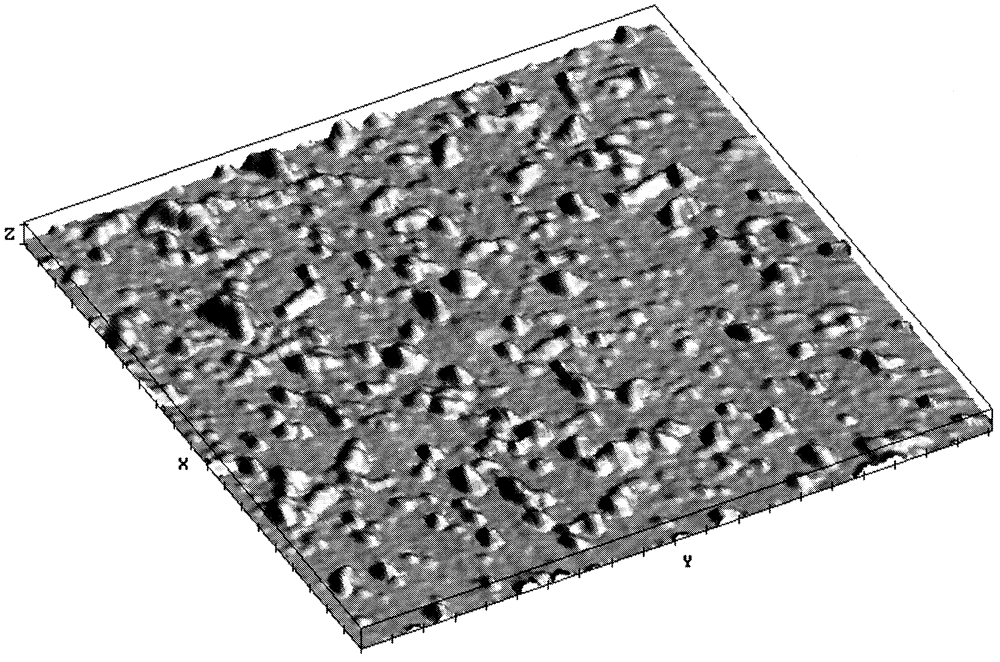

Fig. 4. An AFM image of silver implanted surface of float glass after laser annealing. The *X* and *Y* scales are 100 nm, and the *Z* scale is 40 nm.

30 nm and a full width at half maximum of 13.37 channels (Fig. 2). After annealing, the concentration peak position was not moved, but the distribution of silver atoms is broadened (21.07 channels) compared with that of the as-implanted sample.

The AFM images of implanted samples are shown in Fig. 3. In the main they agree with the commonly observed [13,14] pictures of implanted metal particles in insulators for this microscopy scale. As seen from these figures, the implanted float glass surface is nearly smooth, but there are a lot of spherical hills on this surface with approximately an average diameter of about 10–15 nm. There are no such protrusions on the non-implanted sample. The reason for the existence of surface hills is assumed to be from a sputtering of irradiated glass during implantation, which leads to non-equivalent ejection of ions of different elements from the surface [15] and, probably, exposes the synthesised nanoparticles in the sub-surface glass. The numerical computer programme TRIM and SUSPRE estimations show that, for the implantation conditions used in the present experiments, the thickness of the sputtered glass layer is typically of the order of tens of nanometers. Hence, it is obvious that synthesised buried metal particles at the initial moment of implantation are close to glass surface in the produced sample. The AFM images of laser annealed samples, with a decreased vertical microscopic scale, are presented in Fig. 4. In this case, it is also possible to see clearly defined hills on the glass surface, but the diameter of these hills, in the image plane, assumed to be silver particles, is smaller, but their height is much larger. The side views emphasise these differences. It is noted that the real size of the features observed with AFM may be smaller than it is possible to see in the AFM images, due to convolution effects between the tip and the analysing surface [16].

4. Discussion

Laser pulses deposit energy into the implanted surfaces, and the near-surface of the bulk material, down to a penetration depth defined by the laser wavelength and the material absorption. The initial coupling mechanism of absorption of the excimer laser light is not thermal, but as excess particle energy through excitation energy of bound electrons, kinetic energy of free electrons and so on. For consideration of optical properties of the synthesised Ag-glass composite it is possible to use the effective-medium approximation [11], because typical sizes of metal particles formed by ion implantation in glass, as seen from Fig. 3 and from the early transmission electron microscopy study [12], are orders of magnitude smaller than the wavelengths of relevant electromagnetic radiation. In such composite materials the silver nanoparticles stimulate optical plasmon absorption and change the dielectric constants of the medium generally in the visible and infrared region of spectra. Consequently for a description of the optical absorption of our materials in the ultraviolet we will use the optical features of the float glass only.

The laser optical response of insulators involves both electronic and ionic contributions to the dielectric function [17]. There are virtually no free (conduction-band) electrons at room temperature. Thus ultraviolet optical absorption in laser-irradiated insulators leads to the creation of electron-hole pairs rather than electron heating. If the laser wavelength is greater than, or equal to, the glass bulk bandgap energy, then the laser–solid interaction is dominated by one-photon transitions. When coupled to the relevant mechanisms for relaxation, this in turn determines the energy and the density of electrons and holes available for radiative and nonradiative recombination. An intense laser pulse absorbed and relaxed into a target material heats the surface layer to a relatively high temperature in only a few nanoseconds [17]. There are thus extreme thermodynamic conditions in the irradiated near-surface region. Knowledge of phase transitions, decomposition temperatures, and physical constants that are well understood close to equilibrium should be viewed only as estimates for these non-thermodynamic situations, and be correlated with experimental results from a variety of characterization techniques.

The most important parameter in understanding thermal effects is the temperature distribution in the material and its development in time. Reasonable first order estimates of the subsurface temperature distribution can be made from solutions to the thermal diffusion equation [17]. As a simplest situation, it is possible to consider the diffusion length $l(t)$

[18], which gives an estimate of the length that heat will diffuse in a time t,

$$l(t) = \sqrt{\frac{kt}{pc}} \quad (1)$$

where k is the thermal conductivity ($k = 0.0095$ W/cm K for soda-lime glass [19]), p is the density of float glass (2.47 g/cm^3), c is the specific heat ($c = 0.84$ J/g K for silicate glass [20]). Eq. (1) indicates how far a significant amount of heat should diffuse during a given amount of time. The diffusion length over the time of the laser pulse is important, as this can affect the energy density, which determines the subsurface heating within the sample, and, hence, the threshold of ablation, if the length is greater than the absorption depth [18]. For a laser pulse duration of 17 ns, as in our case, the diffusion length is ~ 92 nm, which is less than the absorption depth ($1/\alpha$) in float glass, where α is the absorption coefficient of float glass ($\alpha = 2 \times 10^{-1}$ cm^{-1} at the wavelength of 248 nm [21]). Thus, we may conclude that laser light is absorbed primarily within a thin layer near the surface, where the implanted silver nanoparticles are maintained, as the implanted depth, calculated from the TRIM computer code, and as confirmed by earlier electron microscopy data [12], gives the implanted ion distribution depth [3] to be about 40 nm. In the present experiments the laser fluence was lower than the value of the ablation threshold for float glass, which is on the order of 5 J/cm^2 [22], and so we may consider all the changes in structure of the laser irradiated composite as a result of local heating, without extensive desorption of material from the surface.

As the result of this near-surface heating, there are changes in optical spectra (Fig. 1). In practice, for the interpretation of the optical spectroscopy data from the presence of metal nanoparticles Mie theory [23] is often applied [11]. The theory is defined by the size of metal nanoparticles. From Mie theory predictions it is assumed that the long wavelength absorption and reflection is caused by large particles of more than 40-nm diameter, whereas the absorption closer to the ultraviolet is from small ($\sim$ 3–4-nm diameter) particles [2,11]. The changes of the position of the transmittance minimum and the reflectance maximum in optical spectra towards the shorter wavelength (Fig. 1), show the effects of decreasing the silver nanoparticle size during the laser annealing. This assumption is in agreement with AFM measurements (Fig. 4), where it is seen that there are a lot of particles on the annealed surface whose size is smaller than 5 nm.

It is obvious that a major reason for the particle size modification is the temperature pulse produced during interaction of the high power laser pulses with the implanted glasses. Laser pulses drive the surface of an insulator to high temperatures during which time there can be dissolution of metal particles. If this happens, then it will lead to an increasing of the concentration of silver atoms in the near-surface region. However, during the cooling part of the annealing cycle there will be competition from new nucleation and regrowth of particles. Rapid cooling from high temperature, after the laser pulse, may freeze in the thermodynamic conditions appropriate to this high temperature and retain metastable phases where the silver atom concentration exceeds the solubility value in the glass. In this case the possibility of regrowth of metal particles will depend on a competition between regrowth and cooling speeds. Hence some regrowth is inevitable.

As was estimated earlier [24], the temperature at the surface of laser annealed float glass reaches values exceeding 1000°C. Under these conditions there is a possibility of melting small silver particles, not least, because their melting temperature is drastically decreased to $\sim$ 400°C for sizes < 30 nm, compared with the bulk metal melting temperature of 960°C [25]. As far as the solid–liquid transition of small particles is concerned, the main factor is the dependence of Laplace pressure on size and interfacial energies [26]. The equilibrium equation leads to the lowering of the melting temperature with size, a phenomenon initially known as ‘thermodynamic size effect’. The phenomenological theories all lead to the relationship $1 - T_{\mathrm{melt}}/T_{\mathrm{bulk}} \approx r^{-1}$, where T_{melt} is the melting temperature particles with radius r, and T_{bulk} is the bulk melting temperature [26]. Therefore, during the excimer laser annealing, the nanoparticles, in principle, can melt and become atomically dispersed silver within the glass.

As seen from the present data the results of high-power KrF laser treatment for the conditions used is to form smaller silver particles in the im-

planted layer of the float glass. Increasing the total laser fluence up to 2 J/cm^2 produces an additional shift of the location of the transmittance minimum and reflectance maximum to smaller wavelengths, with some reduction of intensity. In the case of laser annealing with ArF laser pulses [8] at 193 nm, only decreasing intensities, without any obvious changes in the position peak, were discussed. In spite of this, in both KrF and ArF laser treatment, the high energy pulse power increased the surface temperature of implanted glass and the dominant effects are not essentially different for the two laser frequencies. During ArF laser annealing heating and cooling processes were derived from a 10-Hz repetition rate and single pulse energies of 85 mJ/cm^2. Multiple laser pulses have not resulted in regrowth of metal particles. The glass and metal nanoparticle melting was possible during the entire period of the ArF laser annealing pulse, and above powers of about 500 mJ/cm^2 a total dissolution of silver was determined [8]. In comparison to the ArF study [8], the higher power and low repetition rate of the KrF pulses here, may provide conditions of particle regrowth. Higher KrF laser fluence is not valuable in this context as although it might result in a full dissolution of the silver particles it would also result in ablation and desorption of silver from the implanted float glass.

All these processes depend on a variety of irradiation conditions, such as wavelength of excitation, the pulse repetition rate, the pulse duration, the properties of irradiated material, etc. As seen from the RBS (Fig. 3) data the laser modification of implanted glasses is accompanied by the loss of silver from the implanted layer. This is not a laser stimulated desorption effect, but it is caused by evaporation of silver atoms from the heated surface of the glass [2], together with some diffusion to the surface and into the interior of the glass. The silver accumulated effect on the laser irradiated surface of float glass are seen by AFM (Figs. 3 and 4). Probably, there is some desorption of glass material under the laser pulses, which exposes the silver particles. The loss of silver from the samples reduces the metal atom concentration in the glass, and can be one of the reasons causing a decrease of intensity of optical absorption bands after laser annealing. Nevertheless, there is a clear trend in which large silver nanoparticles are dissolved by the laser pulses.

5. Conclusion

Ion implantation of metal into insulators leads to an excess of the metal, which is unstable in the form of dispersed atoms, so the systems relax into precipitates of metal nanoparticles. As formed, there is invariably a very wide distribution of nanoparticle sizes which degrade the performance for non-linear responses and confuse the interpretation of the fundamental processes. As shown here, the ion implantation and subsequent high power excimer laser pulse treatments may be used to dissolve, and/or regrow, the nanoparticles. Overall this results in a tighter distribution of small particles. The silver-insulator composite material is complex, and so a much wider range of laser pulse conditions, and more data on the cooling rates are required to fully model the changes in the size distributions which can occur.

Acknowledgements

We are grateful to the Royal Society/NATO/97A Postdoctoral Fellowship Programme for financial support of Dr. A. Stepanov at University of Sussex, UK and also to Brite Euram contract BE 4427 (AMENIDAD). Also we wish to thank Yu.N. Osin for help with the supporting experiments.

References

[1] G.W. Arnold, J. Appl. Phys. 46 (1975) 4466.
[2] G.W. Arnold, J.A. Borders, J. Appl. Phys. 48 (1977) 1488.
[3] P.D. Townsend, P.J. Chandler, L. Zhang, Optical Effects of Ion Implantation, Cambridge Univ. Press, Cambridge, 1994.
[4] R.F. Haglund Jr., L. Yang, R.H. Magruder III, C.W. White, R.A. Zuhr, L. Yang, R. Dorsinville, R.R. Alfano, Nucl. Instrum. Methods B 91 (1994) 493.
[5] P.D. Townsend, J. Olivares, Appl. Surf. Sci. 109/110 (1997) 275.
[6] F. Gonella, G. Mattei, P. Mazzoldi, E. Cattaruzza, G.W. Arnold, G. Bertoncello, R.F. Haglund Jr., Appl. Phys. Lett. 69 (1996) 3101.
[7] A.A. Bukharaev, A.V. Kazakov, R.A. Manapov, I.B. Khaibullin, Sov. Phys. Solid State 33 (1991) 578.
[8] R.A. Wood, P.D. Townsend, N.D. Skelland, D.E. Hole, J. Barton, C.N. Afonso, J. Appl. Phys. 74 (1993) 5754.
[9] M. Von Allmen, Laser Beam Interactions with Materials, Springer, Berlin, 1987.

[10] F. Lamouroux, N. Can, P.D. Townsend, B.W. Farmery, D.E. Hole, J. Non-Cryst. Solids 212 (1997) 232.
[11] U. Kreibig, M. Vollmer, Optical Properties of Metal Clusters, Springer-Verlag, Berlin, 1995.
[12] L.C. Nistor, J. van Landuyt, J.B. Barton, D.E. Hole, N.D. Skelland, P.D. Townsend, J. Non-Cryst. Solids 162 (1993) 217.
[13] D.O. Henderson, R. Mu, Y.S. Tung, M.A. George, A. Burger, S.H. Morgan, C.W. White, R.A. Zuhr, R.H. Magruder, J. Vac. Sci. Technol. B 13 (1995) 1198.
[14] A.A. Bukharaev, V.M. Janduganov, E.A. Samarsky, N.V. Berdunov, Appl. Surf. Sci. 103 (1996) 49.
[15] P.D. Townsend, J.C. Kelly, N.E.W. Hartley, Ion Implantation, Sputtering, and their Applications, Academic Press, London, 1976.
[16] A.A. Bukharaev, D.V. Ovchinnikov, E.F. Kukovitskii, N.I. Nurgazizov, N.A. Sainov, Phys. Solid State 39 (1997) 1846.
[17] J.F. Ready, Effects of High-Power Laser Radiation, Academic Press, London, 1971.
[18] J.C. Miller, R.F. Haglund (Eds.), Laser Ablation and Desorption: Experimental Methods in the Physical Sciences, Academic Press, San Diego, 1998, p. 343.
[19] Handbook of Chemistry and Physics, CRC Press, London, 1994, pp. 12–145.
[20] G.W.C. Kaye, T.H. Laby, Tables of Physical and Chemical Constants, Longman, London, 1973, p. 55.
[21] B.G. Bardley, W.G. French, Am. Ceramic Soc. Bull. 52 (1973) 701.
[22] C. Buerhop, B. Blumenthal, R. Weissmann, N. Lutz, S. Biermann, Appl. Surf. Sci. 46 (1990) 430.
[23] G. Mie, Ann. Phys. 25 (1908) 377.
[24] A.L. Stepanov, D.E. Hole, P.D. Townsend, Nucl. Instr. & Methods B, 1998, in press.
[25] T. Castro, R. Reifenberger, E. Choi, R.P. Andres, Phys. Rev. B 42 (1990) 8548.
[26] R. Kofman, P. Cheyssac, A. Aouaj, Y. Lereah, G. Deutscher, T. Ben-David, J.M. Penisson, A. Bourret, Surf. Sci. 303 (1994) 231.